CLINICAL AND EXPERIMENTAL
OPTOMETRY

RESEARCH PAPER

Reconciling visual field defects and retinal nerve fibre layer asymmetric patterns in retrograde degeneration: an extended case series

Clin Exp Optom 2017; 100: 214–226 DOI:10.1111/cxo.12478

Barbara Zangerl[*†] PhD DVM
Andrew Whatham[*†a] DPhil BOptom PGCertOcTher
Juno Kim[†] PhD BSc
Agnes Choi[*†] MOptom PGCertOcTher
Nagi N Assaad[*‡] MBBS MBiomedE
Michael P Hennessy[*‡] MBBS MBiomedE FRAZCO
Michael Kalloniatis[*†] PhD MScOptom FAAO

*Centre for Eye Health, Sydney, New South Wales, Australia
†School of Optometry and Vision Science, The University of New South Wales, Kensington, New South Wales, Australia
‡Ophthalmology Department, Prince of Wales Hospital, Randwick, New South Wales, Australia
[a]Author included posthumously
E-mail: mkalloniatis@cfeh.com.au

Submitted: 14 March 2016
Revised: 21 July 2016
Accepted for publication: 1 August 2016

Background: Accurate diagnosis in patients presenting with lesions at various locations within the visual pathway is challenging. This study investigated functional and structural changes secondary to such lesions to identify patterns useful to guide early and effective management.

Methods: Over 10,000 records from patients referred for optic nerve head assessment were reviewed and 31 patients with a final diagnosis of likely neuropathic lesions posterior to the eye were included in the current study. Fundus photographs, optic coherence tomography images and visual field tests were evaluated for changes with respect to retinal nerve fibre layer topography and prediction of structure-function paradigms. Emerging clinical patterns were examined for their consistency with the likely anatomical origin of the underlying insult in the presence of varying diagnoses.

Results: Data from patients with lesions along the visual system allowed identification of retinal nerve fibre layer asymmetry correlated with visual field defects and ganglion cell analysis. Bilateral discordance in retinal nerve fibre loss easily discernible from an altered pattern of the temporal-superior-nasal-inferior-temporal curve was characteristic for post-chiasmal lesions. These sometimes-subtle changes supported diagnosis in cases with multiple aetiologies or with ambiguous visual field analysis and/or ganglion cell loss.

Conclusion: Intricate knowledge of the retinal architecture and projections allows coherent predictions of functional and structural deficits following various lesions affecting the visual pathway. The integration of adjunct imaging and retinal nerve fibre layer thinning will assist clinicians to guide clinical investigations toward a likely diagnosis in the light of significant individual variations. The case series presented in this study aids in differential diagnosis of retrograde optic neuropathies by using retinal nerve fibre layer asymmetric patterns as an important clinical marker.

Key words: ganglion cells, optic nerve head, optical coherence tomography, retinal nerve fibre layer, retrograde degeneration

Optic neuropathies comprise a group of degenerative disorders of diverse aetiologies that are characterised by the loss of retinal ganglion cells. Accurate diagnosis is complex due to variability and overlap in clinical signs and symptoms, as well as the delay between original pathology and visual manifestation at the optic nerve head. Acute injury to the retinal ganglion cells might take four to six weeks for visible clinical manifestation of optic atrophy (pale optic disc) but can be prolonged with peripapillary retinal nerve fibre layer loss.[1] Conditions caused by cortical insults resulting in retrograde degeneration may emulate retinal nerve fibre layer and visual field defects typically expected with slowly progressing chronic conditions.[2–6] Even changes to the optic nerve head classically expected with glaucoma or arteritic anterior ischaemic optic neuropathy, such as cupping,[7] have been associated with multiple other aetiologies.[8–10] Yet, accurate diagnosis is pivotal in primary eye care for appropriate and timely management to curtail potentially significant threats to vision or mortality, from conditions ensuing from optic neuropathies potentially leading to retrograde degeneration. Therefore, structural assessment guiding differential diagnoses can not necessarily rely solely on stereoscopic fundoscopy, the current gold standard and recommended clinical procedure of choice.[11] Reliable and reproducible neuro-imaging techniques, such as optical coherence tomography (OCT),[12] computerised tomography and magnetic resonance imaging,[13] significantly improve diagnostic abilities.[14,15] Of these, OCT is widely adopted in primary ophthalmic practice and may assist in the differentiation of optic neuropathies.[16,17]

A first understanding of the relationship between visual function and brain lesions originated from the charting of war-related head injuries,[18] subsequently refined, with the help of newly developed technologies, producing a comprehensive map of insults to the visual cortex and corresponding

visual field defects.[19] More specifically, degeneration of grey matter in the temporal and occipital regions of the brain is associated with ganglion cell and inner plexiform layer thinning[20] but typically does not affect the inner nuclear layer.[21] Anatomically, retrograde degeneration is observed as direct retrograde degeneration, when axonal or terminal lesions posterior to the eye up to the lateral geniculate nucleus lead to deterioration of the affected axons back to the retinal ganglion cell bodies in the eye from whence they originate.[22,23] In contrast, trans-synaptic (trans-neuronal) retrograde degeneration ensues from primary lesions past the lateral geniculate nucleus up to and including the primary visual cortex. Clinically, all post-chiasmal retrograde degenerations manifest as bow-tie atrophy on the contralateral side to the lesion and temporal pallor on the ipsilateral side,[24] resulting in congruous visual field loss that should correspond with a homonymous pattern of retinal nerve fibre loss over time, with longevity of the lesion. Due to the frequent and poorly understood variability in observed retinal nerve fibre and visual field defects[2,5,25] retinal ganglion cell loss is often preferred as a clinical marker for diagnosis.[26,27] Furthermore, the retinotopic location of retinal nerve fibre axons entering the optic nerve head can cause early changes to be concealed from clinical observation, visual field testing or OCT peripapillary retinal nerve fibre layer profiles, despite being readily observed in macular ganglion cell measures. Therefore, a number of recent studies provided strong arguments to perform ganglion cell analysis in patients with suspected retrograde degeneration to take advantage of the concordance with visual field loss for diagnosis.[4,26,28,29]

Injuries at the chiasm are somewhat unique in triggering a particularly characteristic defect, termed band optic atrophy, which affects ganglion cells nasal to the optic disc and fovea.[30] Typically, corresponding visual field defects are described as temporal hemianopia, with the exact extent dependent on the site and size of the chiasmal depression.[31,32] While retinal nerve fibre loss was recently confirmed as an excellent predictor of visual outcome after pituitary decompression,[33] it is not well correlated with band optic atrophy.[34] We performed an extensive case study to identify commonalities in visual field, retinal nerve fibre layer and ganglion cell changes caused by retrograde degeneration and ascertain clinically relevant features to guide differential diagnosis in primary eye care.

METHODS

The Centre for Eye Health (CFEH) provides testing and diagnostic services to local eye care providers on a referral-only basis.[35] Of 10,451 patients aged 18 to 80 years seen between January 2010 and August 2015 at CFEH, 34 (0.3 per cent) were diagnosed by the attending optometrist and consulting ophthalmologist with optic neuropathy secondary to lesions posterior to the eye. Patients with a spherical equivalent worse than −3.00 D were excluded from the study to avoid any potential bias due to myopic changes of the optic nerve head. Written consent was obtained from 31 patients following the tenants of the Declaration of Helsinki and approved by the Biomedical Human Research Ethics Advisory Panel of the University of New South Wales in Australia. Diagnoses for these patients were re-evaluated by a general ophthalmologist and retina specialist and provide the basis for the current series of cases. To discern clinical components relevant to retrograde degeneration resulting from the original insult, patients with a diverse range of individual diagnoses were divided into groups by pathology affecting distinct locations of the visual pathway (Table 1).

Clinical data on all cases were carefully reviewed to develop a better understanding of the spectrum of defects of the visual field, retinal nerve fibre layer and retinal ganglion cells expected with retrograde degeneration and their correlations. In short, we used a 'reverse mapping' approach (for details see case 1) mapping visual field defects onto the specific organisation, in which ganglion cell fibres enter the optic nerve to plot retinal nerve fibre loss.[36,37] An accurate and complete diagnosis pertaining to the presented cases was obtained wherever possible. Due to the unique position of CFEH as a referral-only centre and the consequent onus of care residing with the referring practitioner, patients were not always able or willing to disclose the exact nature of their original diagnosis. Information pertinent to the presented cases was provided as detailed as available (Table 2, Table S1). The case series resulted in the development of a schematic representation of clinical changes expected with retrograde degeneration secondary to dysfunction in various parts of the visual pathway.

Location	Pathology	Number of cases
Pre-chiasmal unilateral optic neuritis/atrophy	Multiple sclerosis/Divic's disease	4
	Trauma	3
	Unknown	5
Chiasmal	Confirmed pituitary tumour	1
	Unconfirmed	3
Post-chiasmal retrograde degeneration	Cardiovascular accident†	6
	Trauma	3
	Surgery	1
	Viral	1
	Unknown†	4

†The retinal nerve fibre layer/ganglion cell thickness was above average in five patients (four cardiovascular accident patients and one with unknown pathology). While these patients had described asymmetry, the absolute measurements remained within normal limits.

Table 1. Classification of 31 clinical cases with retrograde degeneration

RESULTS

Case 1: detailed work-up of a retrograde degeneration case study

CORRELATING VISUAL FIELD, RETINAL GANGLION CELL AND RETINAL NERVE FIBRE LOSS

Ferreras and colleagues[37] predicted the clock hour position of the associated fibres entering the optic nerve head for each point of the standard 24–2 Swedish

Patient number	Age	Sex	VA		SE		Relevant symptoms/history	Lesion location	Pathology
			RE	LE	RE	LE			
1	38	M	6/7.6	6/6	−0.50	−0.63	Meningitis at 2 weeks old	Left calcarine fissure	Inflammation
2	57	M	$6/6^{+2}$	6/4.8	−0.38	−0.25	Surgical removal of an aneurysm at 39 years	Left optic tract	Aneurysm/ surgery
3	51	M	$6/6^{-1}$	6/6	+0.25	+0.13	Fractured right eye socket at 41 years and motorcycle accidents with head injuries	Right post-chiasm	Head trauma
4	55	M	6/6	6/6	+0.00	+0.00	Previous chemical trauma, nothing else, suspected glaucoma	Optic tract	Unknown
5	69	M	6/6	6/4.8	+2.75	+2.75	Transient ischemic attack at 60 years	Post-chiasm	Mini-stroke
6	24	M	$6/6^{+2}$	$6/6^{+2}$	+0.00	+0.25	Unremarkable, LE pigmented lesion	Right post-chiasmal, most likely occipital lobe	Unknown
7	23	M	6/6	6/6	+0.63	+0.63	Head injury at 2 years of age, first imaged at 19, no change since	Left post-chiasmal, most likely occipital lobe	Unknown
8	60	F	$6/4.8^{-1}$	6/4.8	+0.63	+0.25	Diagnosed with multiple sclerosis at 33 years, left optic neuritis at 43 years	Left optic nerve	Optic neuritis LE
9	84	M	6/120	6/15	−1.50	−2.00	Pituitary tumour diagnosed at 74 years	Optic chiasm	Pituitary tumour
10	54	M	$6/6^{-2}$	6/6	−0.75	−0.50	Blurry vision, referred for macula and glaucoma suite	Likely left optic chiasm	Unknown
11	51	M	6/12	6/75	−0.50	−1.00	LE poor vision for 3 years, resident ophthalmologist and optometrist consulted in last 6 months with no results	Likely optic chiasm	Unknown
12	69	M	6/5	6/5	+0.25	−1.25	Transient double vision 6 months ago followed by partial visual loss	Left occipital lobe and both optic nerve heads	Glaucoma; CVA
13	75	F	6/6	6/6	−0.63	−1.50	Electrical injury at 66 years; Cardiovascular accident at 70 years	Likely right parietal lobe	Electrical injury; CVA
14	77	M	6/9	6/9	+1.00	+0.75	Cardiovascular accident at 62 years	Likely right temporal lobe	CVA

CVA: cardiovascular accident, SE: spherical equivalent, VA: visual acuity.
Patient 1: Features are shown in Figures 1 and 2.
Patients 2 to 7: Features are shown in Figure 3.
Patients 8 to 11: Features are shown in Figure 4.
Patients 12 to 14: Features are shown in Figure 5.

Table 2. Patient characteristics

interactive thresholding algorithm visual field (Figure 1A, B, F and G), which was subsequently stylised (Figure 1A1, B1, F1 and G1). Thus, any deficit in the visual field test should be associated with a loss of retinal nerve fibres at the corresponding position(s) and assist with detailed diagnosis of observed retinal nerve fibre loss. We further expanded this model by using information on the relative number of fibres described by Ferreras and colleagues[37] for individual clock hour sectors and the total central retinal draft area for each fibre bundle to estimate the relative impact of such loss in relation to the total number of fibres present at each location (Figure 1B and G). Of note, based on the limitations in size and resolution of the visual field test used for this predication, the current model does not provide information on clock hours four and nine. With regard to clock hour nine, it is commonly accepted that the retinal nerve fibre layer at this location comprises axons derived from macular ganglion cells. Consequently, we included this clock hour in our model predicting significant retinal nerve fibre loss with macular damage (Figure 1B and G, grey arrows).

A temporal loss of vision in the right eye of a 38-year-old male patient (Patient 1, Figure 1A) was mirrored in the corresponding thinning of the nasal ganglion cell complex (Figure 1C) in concordance with the above-developed model. Affected nerve fibre bundles predicted to be interspersed with unaffected bundles (Figure 1B1) are clinically manifested in an irregular pattern of retinal nerve fibre loss (Figure 1E). This loss was predominantly visible nasal to the macula (Figure 1D2), an area that is not represented in a standard visual field, as it corresponds approximately to the horizontal midline.[36]

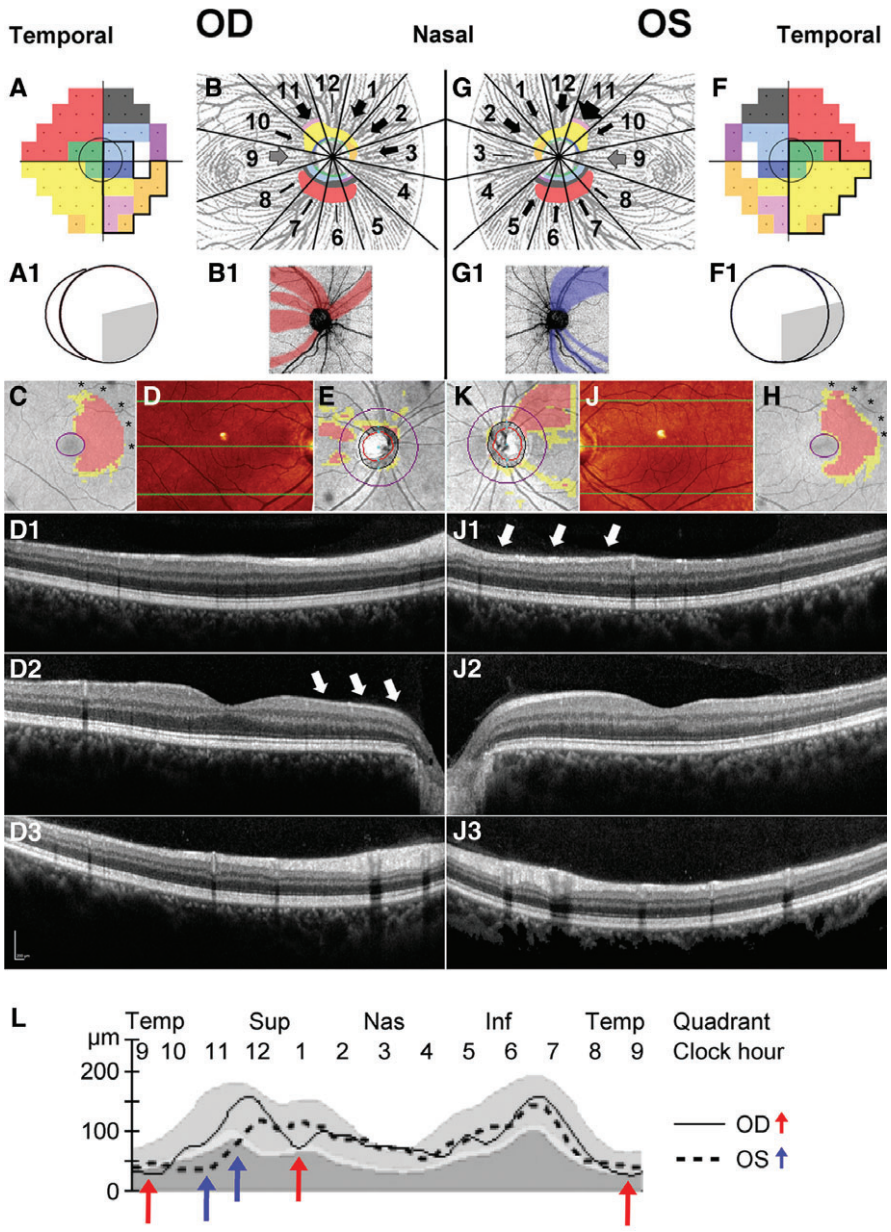

Figure 1. Reconciling retinal ganglion cell and retinal nerve fibre layer loss from retrograde degeneration. The visual field defect observed in Patient 1 (A and F, black outline) was projected onto a visual field map with marked coloured areas of the retinal nerve fibre layer adapted from Ferreras and colleagues.[37] The central grey circle corresponds to the area assessed by ganglion cell analysis. Following the map proposed by Ferreras and colleagues,[37] the approximate thickness of nerve fibre bundles from individual visual field areas are visualised for each sector of the retinal nerve fibre layer by the equivalent colour (B and G). The estimated amount of loss was illustrated by the thickness of black arrows for each affected sector. The grey arrow indicated the likely affected macular bundle, which has no matching visual field points.[36] Both the visual field defect and the position of associated thinning of the retinal nerve fibre layer were subsequently stylised (A1, B1, F1, G1). Ganglion cell analysis deviation maps mirrored the visual field defect within the imaged central seven to eight degrees in both eyes; the macular defect may extend well beyond this area (C and H asterisks). Optical coherence tomography scans through the posterior pole (D and J). Retinal profiles are provided along the three green horizontal lines corresponding to locations in the superior (D1), central (D2) and inferior (D3) macula. Based on the localisation of ganglion cell loss, drop out from the retinal nerve fibre layer is most marked nasal of the right (D2, white arrows) and superonasal of the left macula (J1, white arrows). Observed thinning of the retinal nerve fibre layer (E, K), generally following the patterns predicted in B, B1 and G, G1. L. Asymmetry in the retinal nerve fibre layer temporal-superior-nasal-inferior-temporal (TSNIT) curve (L) highlights thinning of the temporal and superonasal aspects contralateral (RE, red arrows) and superotemporal aspect ipsilateral (LE, blue arrows) to the original cortical insult (Figure 2).

Corroborating the predicted pattern, the nasal visual field defect of the left eye (Figure 1F) is associated with a thinning of the temporal ganglion cell complex (Figure 1H) and a corresponding arcuate nerve fibre bundle loss (Figure 1K) with the majority of thinning apparent superotemporal to the optic nerve head (Figure 1J1). Combined nerve fibre loss for both eyes results in discordant asymmetries of the undulating pattern in the temporal-superior-nasal-inferior-temporal (TSNIT) curve (Figure 1L), with thinning in sectors 11 and possibly 5 in the eye ipsilateral (left eye, Figure 1L, blue arrows) and sectors 9 and potentially 1 thinned in the eye contralateral (right eye, Figure 1L, red arrows) to the original brain lesion.

INTEGRATION OF FINDINGS TO ARRIVE AT A DEFINITIVE DIAGNOSIS FOR PATIENT 1

Patient 1 was first referred for glaucoma assessment due to asymmetric optic nerve cupping (right more than left) and distinct superior retinal nerve fibre bundle loss in the left eye. Optic nerve head assessment for this and all subsequent patients included patient's medical and family history, age, gender, visual acuity, relevant symptoms, patient history and known or inferred lesion location and pathology, slit-lamp examination and funduscopy. Stereoscopic optic disc images and posterior pole fundus images were obtained through dilated pupils with a non-mydriatic fundus camera (Kowa nonmyd WX 3D Stereo Fundus Camera; Kowa, Tokyo, Japan) and reductions in the peripapillary nerve fibre layer were qualitatively discerned with direct clinical visualisation (Figure 2A and B). Quantitative measurement was confirmed using spectral domain OCT images from a Cirrus OCT (Cirrus HD-OCT 4000, version 7.0; Carl Zeiss Meditec, Dublin, California, USA) acquired with the optic disc cube 200 × 200 protocol centred on the optic disc (Figure 2C and D). Visual field tests taken with the Humphrey Field Analyzer 750 (Zeiss/Humphrey Systems, Dublin, California, USA) and Goldmann perimetry (MT-325UD projection perimeter; Takagi Ophthalmic Instrument Europe Ltd, Manchester, UK) appeared congruous and respecting the vertical meridian, highly suggestive of post-chiasmal retrograde degeneration (Figure 2E and F). Of note, visual field tests with the Humphrey Field Analyzer were generally considered reliable, if they were completed with less than 20 per cent fixation loss, false-negative or false-positive error. While the optic nerve head and retinal nerve fibre layer changes were non-symmetric and in potential discordance with the visual field defect, retinal ganglion cell analysis obtained with the same Cirrus OCT using the Macular Cube 512 × 128 protocol centred on the macular for ganglion cell analysis corroborated a non-glaucomatous aetiology (Figure 2G and H). Upon further questioning, the patient reported having suffered meningitis at two weeks of age resulting in a cortical lesion at the left calcarine fissure, diagnosed at 16 years of age (Figure 2I). Based on the concordance of clinical findings with the developed correlation between visual field defects and nerve fibre loss, the infantile meningitis insult was identified as the sole reason for the observed clinical features.

Cases 2 to 7: clinical presentation of post-chiasmal retrograde degeneration

Half of all patients (15 of 31) included in this study displayed clinical signs consistent with post-chiasmal lesions (Table 1). Six representative cases are shown to demonstrate variability in presentation and highlight common features (Table 2, Figure 3). A suggested homonymous pattern of visual field defects was generally indicative of post-chiasmal lesions (Figure 3D), although OCT imaging proved comparatively more sensitive and has the added advantage of being an objective procedure (Figure 3E and F). In addition to the congruous changes in visual field defects and retinal ganglion cell loss, patients with confirmed post-chiasmal lesions always exhibited the described discordant asymmetry pattern in the TSNIT curve caused by the differences between the eyes in the location of retinal nerve fibre layer thinning (Figure 3C, highlighted by arrows in Patients 2 and 3) with few or no regions affected by bilateral depression. The consistency between expected ganglion cell analysis and retinal nerve fibre patterns supported diagnosis of retrograde degeneration even in the absence of marked reductions in the visual field at the time of examination (Figure 3D, Patient 4). A right inferior quadrantanopia observed in Patient 5 was suggested by the visual field test results and the ganglion cell analysis (Figure 3D–F). The matching, yet subtle corroborating changes in the retinal nerve fibre layer (Figure 3B) could easily be overlooked without intricate knowledge of the underlying correlation. This is even more important as individual patients may display significant thinning of the retinal nerve fibre layer, which is not necessarily flagged as statistically significant in comparison to a normative range. Retinal nerve fibre layer thinning was much more pronounced in both Patients 6 and 7 (Figure 3B and C).

Cases 8 to 11: clinical presentation of pre-chiasmal and chiasmal lesions

Anterior chiasmal syndrome, commonly induced by tumours of the pituitary gland and less frequently by craniopharyngioma and pre-chiasmal conditions can largely vary in the expression of retinal nerve fibre layer thinning depending on the main site of damage. Diagnosis of pre-chiasmal lesions is signified by either unilateral structural and/or functional loss supported by compatible patterns of visual field deficit and nerve fibre loss and patients typically presenting with various other clinical signs and symptoms. Due to the large variations in clinical presentation and the frequent presence of other diagnostic symptoms, we have only provided one representative case and detailed analysis (Figure 4, Patient 8).

In contrast, diagnosis of chiasmal insults, while relatively rare, is particularly critical as visual defects may be the earliest symptom of disease. Patients identified during this study varied from subtle unilateral changes to extended bilateral field defects with preferential temporal loss (Figure 4, Patients 9 to 11). The specific anatomical basis of the nerve fibre layer contributing to temporal visual field loss explains why chiasmal lesions are particularly difficult to identify through retinal nerve fibre layer analysis. A bilateral, 'star-like' pattern of retinal nerve fibre layer thinning was present in all reviewed cases (Figure 4B), which would be predicted due to the spread in nerve fibre bundles damaged by lesions at or around the chiasm. Optic disc pallor was present only in Patient 9 with established pituitary gland tumour for over 10 years, most prominently in the right eye (Figure 4A). Diagnosis of chiasmal lesions from ganglion cell analysis and visual fields was particularly difficult in cases with early changes (Patient 10), when the affected

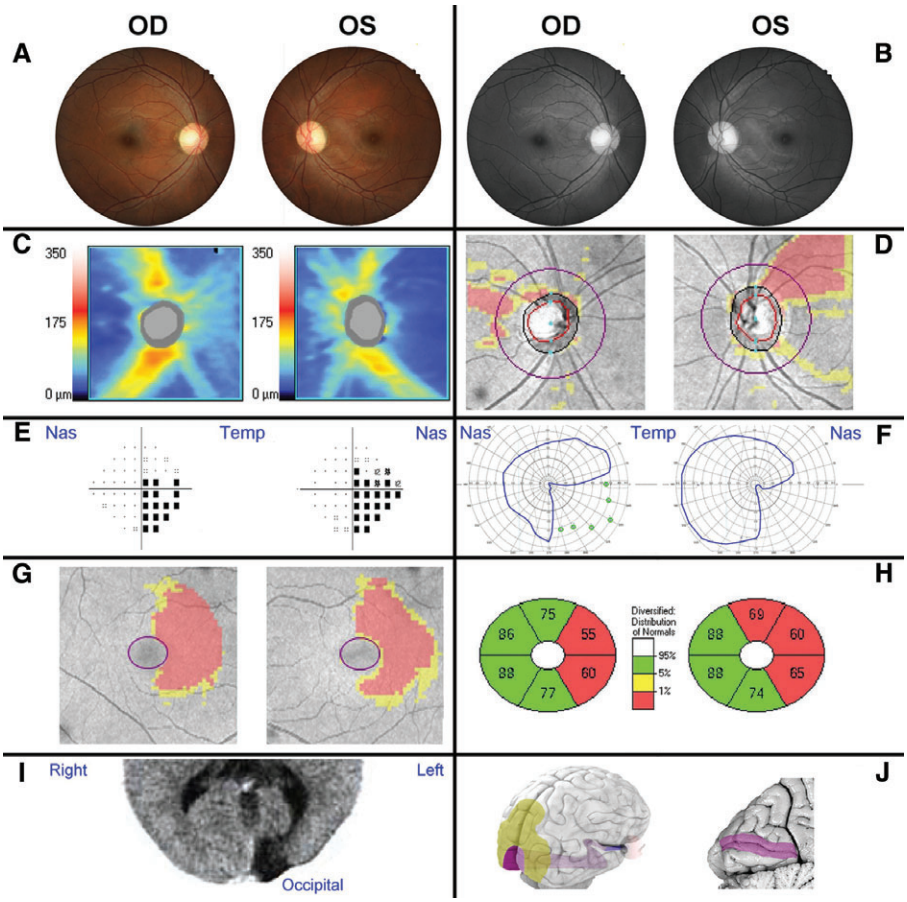

Figure 2. Clinical examination of a 38-year-old male patient with neuropathy. Patient 1 had no systemic conditions, relevant family and/or medical history. Visual acuity (6/7.6 R, 6/6 L) and intraocular pressures (15 mmHg OU) were near normal range and no relative afferent pupil defect was present. A. The patient presented with a possible temporal pallor of the optic nerve head and slight superior sloping of the left retinal rim. B. Red-free photography of the posterior pole further indicated superotemporal retinal nerve fibre drop-out consistent with a potential arcuate defect. C, D. The retinal nerve fibre layer defects were confirmed by optical coherence tomography images, as shown by the thickness heat map (C) and deviation map (D). E–H. A central 24–2 threshold visual field test identified a right inferior quadrantanopia (pattern deviation), which was corroborated by the restricted pattern obtained with Goldmann perimetry (F, blue outlines) and agrees with the ganglion cell analysis deviation map (G) and sector thickness analysis (H). I. Computerised axial tomography revealed an area of hyporeflectivity at the left occipital brain pole. J. An overview of the anatomy of the visual system from a right caudolateral view onto the brain illuminates the position of the optic nerve, optic tract and visual radiation (blue/purple) in relation to the eye and visual cortex (purple) and association areas (yellow). A sagittal section through the visual cortex (left side) reveals the calcarine fissure corresponding to the aberrant area in the patient's brain scan.

areas appear random and at a late stage of disease (Patient 11), when the extensive damage masked any particular configuration of damage (Figure 4D–F).

Cases 12 to 14: selected complex cases

Two main obstacles to accurate diagnosis of conditions with ganglion cell loss are comorbidities and interpretation of results with regard to a normal reference. Patient 12 reported an episode of transient double vision six months prior to clinical examination, followed by partial obstruction of vision. A bilateral superior arcuate nerve fibre bundle defect is highly suggestive of glaucomatous neuropathy (Figure 5B) but functional assessment pointed toward a right superior quadrantanopia (Figure 5D) consistent with changes to the inferior optic nerve head margins (Figure 5C, red arrows). Subsequent brain scans confirmed a left inferior occipital lobe lesion. Given the short time since the lesion occurred, the nerve fibre damage may become more pronounced over time, such as in Patient 13, who suffered a cardiovascular accident four years prior to presenting for examination (Figure 5C, red arrow). This case was particularly interesting due the left visual field having been compromised by an electric shock five years before the

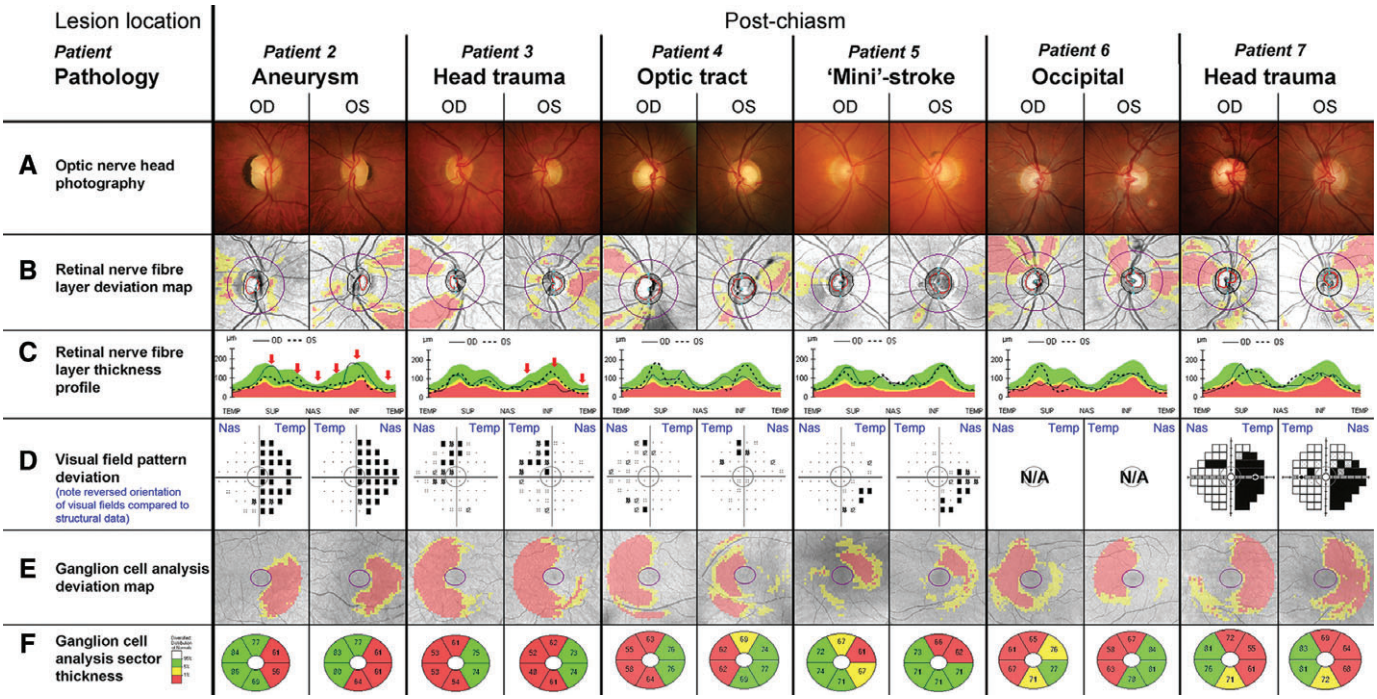

Figure 3. Selected patients with post-chiasmal retrograde degeneration. The central grey circle in each of the visual field pattern deviations (D) corresponds to the area assessed by the ganglion cell analysis (E, F). Please note that conventionally visual field test results (D) are aligned to display the left eye on the left side and the right eye on the right hand side of the observer. As indicated by the blue labels, the opposite order was chosen for this figure to align visual field tests with all other results of the respective eye, resulting in a reversal of the orientation for this panel only. Additional patient details are provided in Table 2 and in the text. Patient 2. A. Patient 2 had average-sized optic discs with a larger right optic nerve head. The parapapillary pigmented crescent corresponded to congenital retinal pigment epithelial hyperplasia. B, C. The peripapillary nerve fibre layer profile revealed relative reduction in the left superotemporal and inferotemporal quadrants and right temporal, with additional asymmetry due to thinned right supero- and inferonasal regions (C, red arrows). D–F. Visual field tests exposed a nearly complete right-sided homonymous hemianopia consistent with the patient's history of cerebral injury and the left-sided thinning of the ganglion cell layer (E, F). Patient 3. A. Patient 3 displayed a reduction in the inferior neuroretinal rim in the right eye and possibly generalised thinning in the left eye. B, C. The retinal nerve fibre layer was significantly thinned supero- and inferotemporally in the right eye and temporally in the left eye again with the additional asymmetry in the inferonasal area (red arrow). D–F. The incomplete left superior quadrantanopia was consistent with right-sided thinning of the ganglion cell layer (E, F). Patient 4. A. Patient 4 presented average sized to large optic discs with large cupping and possible rim thinning superotemporal and inferotemporal in the right eye. B, C. Retinal nerve fibre layer analysis revealed corresponding superior and inferior loss in the right eye and temporal and inferonasal thinning in the left eye. D–F. A mild homonymous left-sided visual field defect was corroborated by the homonymous right-sided ganglion cell loss (E, F). Patient 5. A. Patient 5 had average-sized discs with moderate beta zone parapapillary atrophy and a slightly larger disc and cup size in the left eye. B, C. Retinal nerve fibre layer analysis revealed reduced thickness temporal in both eyes, superonasal in the right and inferonasal in the left eye. D–F. The incomplete right inferior quadrantanopia was mirrored by the left superior ganglion cell layer thinning (E, F). Patient 6. A. Patient 6 had originally been referred for a hypo-pigmented area inferotemporal of the left optic nerve head, which was diagnosed as small serous detachment in an otherwise unremarkable fundus with average-sized optic discs. B, C. Independent of the original diagnosis, marked thinning of the superotemporal nerve fibre layer in the right eye and temporal nerve fibre layer in the left eye was noted. D. Interestingly, this patient was unaware of any concerns with his vision and, as a consequence, visual fields were not obtained prior to transfer for neurological examination. E, F. Symmetrical thinning of the temporal right and nasal left ganglion cell analysis confirmed a likely occipital lesion followed by retrograde degeneration. Patient 7. A. Patient 7 had average-sized optic discs with medium cupping, which was relatively bigger with thinned superior and temporal neuroretinal rims in the right eye compared to the left. B, C, E, F. Retinal nerve fibre layer and ganglion cell analysis results were essentially a mirror image of those obtained for Patient 6. D–F. Visual field test was obtained with the Humphrey Matrix 715 Visual Field Analyzer (Zeiss/Humphrey Systems, Dublin, California, USA), as specifically requested by the referring practitioner, revealing bilateral inferior right quadrantanopia with additional reduction of the superior right quadrant, confirmed by ganglion cell analysis (E, F).

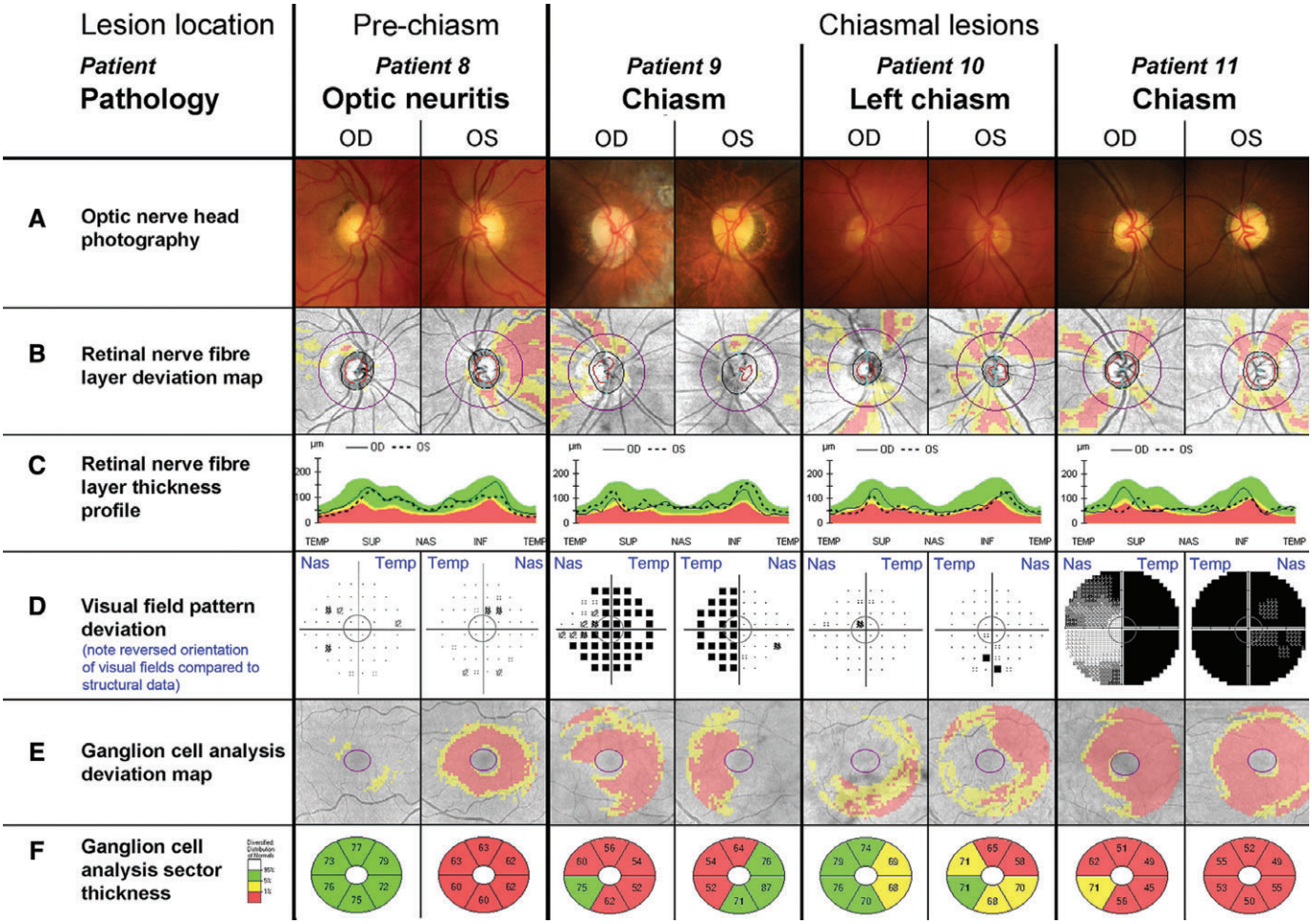

Figure 4. Variation of clinical findings with pre-chiasmal and chiasmal lesions. The central grey circle in each of the visual field pattern deviations (D) corresponds to the area assessed by the ganglion cell analysis (E, F). D. Please note that conventionally visual field test results are aligned to display the left eye on the left side and the right eye on the right hand side of the observer. As indicated by the blue labels, the opposite order was chosen for this figure to align visual field tests with all other results of the respective eye, resulting in a reversal of the orientation for this panel only. Additional patient details are provided in Table 2 and in the text. Patient 8. A–C. Patient 8 presented with an inferiorly thinned neuroretinal rim in the left eye, which was also evident in the retinal nerve fibre layer deviation map next to extensive temporal thinning (B, C). D. Both eyes revealed scattered points of reduced sensitivity in the visual field and the mean deviation was relatively reduced (–1.75 dB) in the left eye. E, F. Ganglion cell analysis showed overall thinning in the left eye. Patient 9. A. Patient 9 had large optic discs with extensive parapapillary atrophy. B, C. The neuroretinal rim and nerve fibre layer reveal superiorly thinning in both eyes and several arcuate areas of thinning of the nerve fibre layer in the temporal aspect of the right eye. D–F. The visual field test indicated bitemporal hemianopia, with the hemianopia in the right eye extending inferonasally. Visual field test results were concordant with the ganglion cell analysis results (E, F). Patient 10. A. Patient 10 presented average discs with intact neuroretinal rim. B, C. The retinal nerve fibre layer profile appeared generally thin, with slight asymmetry between both eyes in the supero- and inferonasal aspects. D. The visual field revealed a focal inferior depression in the left eye, which did not correspond to the bilateral inferior thinning highlighted by the ganglion cell analysis and extended nasally in the left eye (E, F). Patient 11. A. Patient 11 had average sized discs with bilateral pale and atrophic neuroretinal rims. B, C. The retinal nerve fibre layer showed a star-like drop-out pattern in both eyes leading to an undulating temporal-superior-nasal-inferior-temporal (TSNIT) curve. D–F. The patient suffered from a complete temporal visual field defect in the right and almost complete field defect in the left eye, paralleled by extensive loss in ganglion cell thickness (E, F).

cardiovascular accident (Figure 5D) and both retinal nerve fibres and ganglion cell scans staying within normal limits (Figure 5B, E and F). The latter was also true for Patient 14, who had suffered a cardiovascular accident 15 years prior to examination, developed left superior quadrantanopia with macular sparing (Figure 5D), associated asymmetries in the TSNIT curve (Figure 5C) and possible thinning in the ganglion cell analysis sectoral analysis specifically of the left eye (Figure 5F). Due to the variation in retinal nerve fibre layer thickness and loss after injury for individual patients, subtle changes (Figure 5C, red arrow) can support a diagnosis in patients with otherwise little or no structural changes.

DISCUSSION

Reconciling incongruent functional and structural clinical information

Retinal nerve fibre patterns corroborate visual field data for lesions located before and including the optic chiasm but they are discordant between the two eyes and with visual field deficit, if the lesions are post-chiasmal.[4,26,28,29] Retrograde degeneration originating from post-chiasmal lesions results in a homonymous pattern of visual field loss due to the partial decussation of optic nerve axons at the optic chiasm.[25,38] The comprehensive study of presented cases allowed us to extend the known relationship between the site of a lesion and the resulting visual field defect to the corresponding pattern of retinal nerve fibre layer thinning (Figure 6). While there is seemingly large variation in the nerve fibre loss with retrograde degeneration, this reference can be used to guide diagnosis through association of clinical observations with the most likely location(s) of the causative insult.

An important consideration in diagnosing underlying conditions causing associated ganglion cell loss is the time frame within which the respective degeneration occurred and differentiation from expected age-related decrease in retinal nerve fibres. The mean retinal nerve fibre layer thickness decreases more rapidly in patients with homonymous hemianopia during the first 24 months following injury.[5] Due to the wide range of normative data and large variation in the changes to the retinal nerve fibre layer following cerebral insult,[5] reduced thickness may only occur marginally and does not need to fall outside normal limits and thus will not be flagged as significant loss by automated OCT algorithms. This was noted in some of the presented patients, most markedly Patient 14, who showed almost no discernible structural changes 15 years after suffering from a cardiovascular accident. If OCT baseline data were available from patients prior to or at the beginning of such events, changes could be evaluated more accurately for individual patients rather than in comparison to a normative range. The accrual of baseline data from healthy patients would significantly aid in the recognition of later changes, whether disease or age-related and can be used for progression analysis, given the high test-retest reliability of these instruments.[39] As various conditions leading to retrograde degeneration are not exclusive, accurate diagnosis may not always be possible.

The most common differential diagnosis as well as co-morbidity to retrograde degeneration remains the slowly progressive glaucomatous neuropathy.[40] It is not uncommon that patients are initially diagnosed and sometimes treated for glaucoma.[26] OCT measurements could support differential diagnosis in these cases, as well as provide evidence of lesions prior to a recognisable visual field defect.[41] Given that glaucoma originates as a pre-chiasmal disease, the retinal nerve fibre loss should correspond to the visual field loss, although the two eyes often display asymmetry.[42] Based on the retinotopic organisation of retinal axons, areas of reduced vision are expected to respect the horizontal but not the vertical meridian, particularly in the superior and/or inferior aspects in its typical form (Figure S1, Patient 15). We have provided examples in the supplementary materials (Table S1, Figure S1) to highlight typical patterns of glaucomatous patients even in the absence of raised intraocular pressure (Patients 16–18: normal tension glaucoma) or unilateral manifestation (Patient 19). In addition to comorbidities, it has to be noted that the demonstrated structural and functional changes characteristic of retrograde degeneration may be masked by congenital variations of the optic nerve head, such as myopic or tilted discs.

The exact mechanism of retrograde degeneration remains to be elucidated but brain-derived neurotrophic factor is thought to be a key player in the activation of the apoptotic cascade in sensory neurons, both antegrade and retrograde,[43] possibly in combination with increased sensitivity to atrophy due to the loss of neuroplasticity.[44] Consequently, post-synaptic cells from neuronal junctions at the lateral geniculate nucleus can indirectly trigger loss of primary optic nerve cells with the same consequences as direct insults on the optic tract. In addition to well-defined apoptotic pathways (for overview see You and colleagues[45]), the death of pyramidal cells located in layer VI of the visual cortex (Figure 6, green) may contribute to axonal degeneration subsequent to insult along the optic tract. Consequently, the resulting retinal ganglion cell loss closely follows the distinct and well-defined topography of the nerve fibre layer for both eyes and is not a consequence of random effects, such as elevated intracranial pressure, which would produce asymmetric arcuate-like patterns of nerve fibre loss.[46] Thus, distinct features are observed for pre- and post-chiasmal insults leading to retinal ganglion cell loss (Figure 7).

Post-chiasmal retrograde degeneration

- Congruous change in ganglion cell analysis
- Ganglion cell analysis obeys vertical midline
- Discordance of visual field/ganglion cell analysis with retinal nerve fibre layer analysis
- Retinal nerve fibre layer asymmetry, most notably in the supero- and/or infero-nasal aspects.

Pre-chiasmal optic degeneration

- Incongruous change in ganglion cell analysis
- Ganglion cell analysis obeys horizontal midline
- Largely concordance of visual field/ganglion cell analysis with retinal nerve fibre layer analysis
- Often unilateral or areas of bilateral symmetrical retinal nerve fibre layer thinning.

CONCLUSION

We have demonstrated that deviations in the thickness of the retinal nerve fibre layer strictly respect anatomical topography and can help with differential diagnosis of

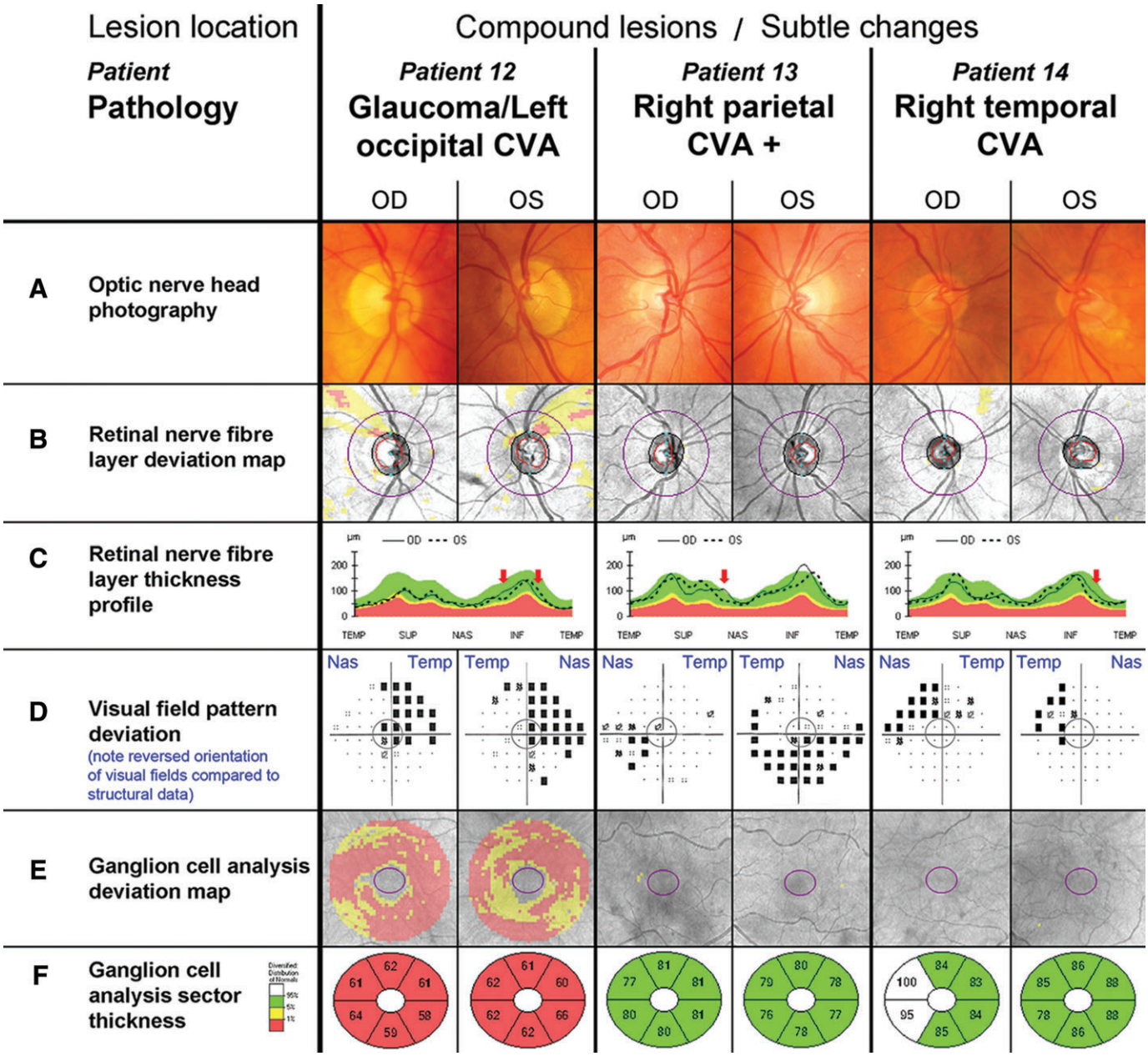

Figure 5. Common, non-classical clinical findings with retrograde degeneration. The central grey circle in each of the visual field pattern deviations (D) corresponds to the area assessed by the ganglion cell analysis (E, F). D. Please note that conventionally visual field test results are aligned to display the left eye on the left side and the right eye on the right hand side of the observer. As indicated by the blue labels, the opposite order was chosen for this figure to align visual field tests with all other results of the respective eye, resulting in a reversal of the orientation for this panel only. Additional patient details are provided in Table 2 and in the text. Patient 12. A–C. Patient 12 had bilateral thin superior neuroretinal rims and beta parapapillary atrophy paralleled in the bilateral arcuate superior nerve fibre defects (B, C). D. The patient's visual field revealed right superior homonymous quadrantanopia. There was superior depression in both eyes and additional inferior nasal depression in the left eye. E, F. Generalised ganglion cell layer thinning was present. Patient 13. A–F. Patient 13 presented with left inferior quadrantanopia, extending temporally in the left eye (D) but no other noticeable abnormalities in the optic nerve head or ganglion cell analysis. Patient 14. A–F. Patient 14 displayed a visual field defect consistent with slightly incongruous left superior quadrantanopia (D), which was not accompanied by any other noticeable changes in the optic nerve head or ganglion cell analysis (A–C, E, F). It should be noted that the right temporal ganglion cell layer appeared thicker than normal (F).

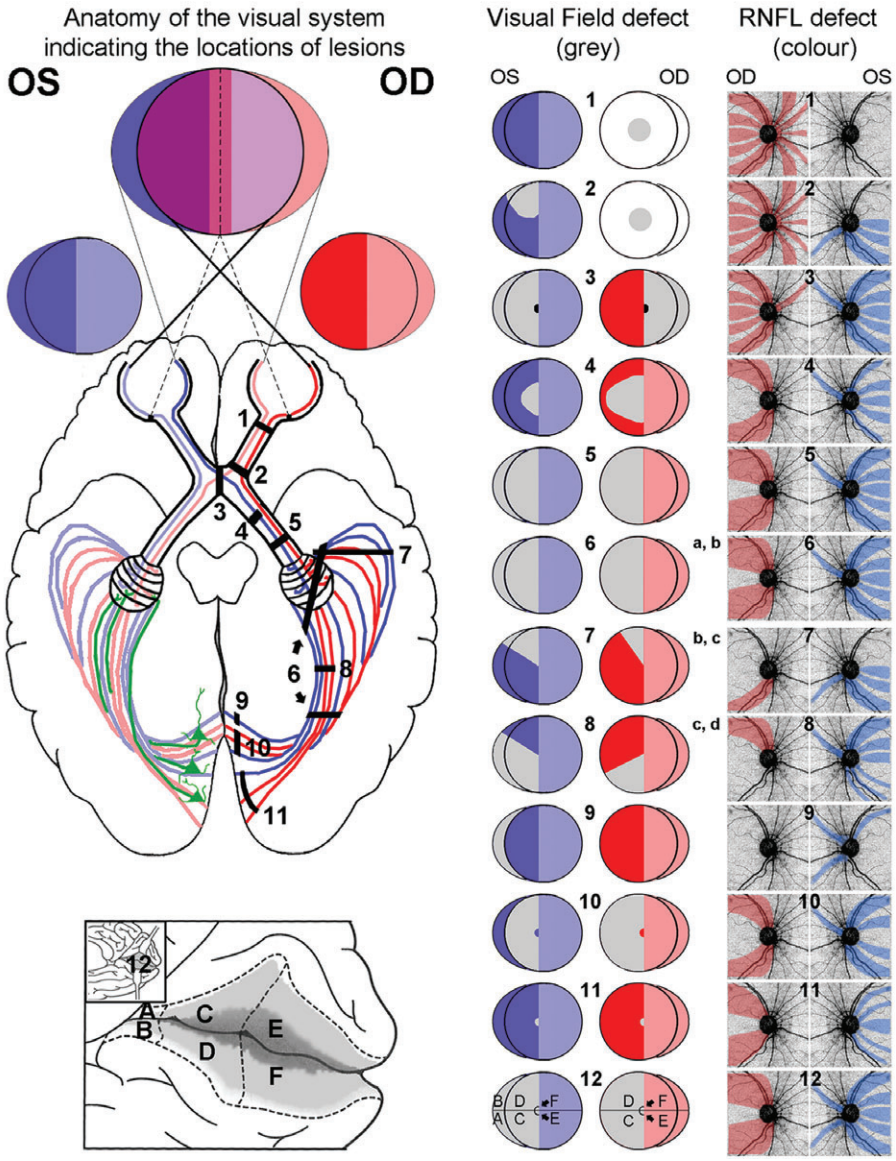

Figure 6. Visual field and retinal nerve fibre defects following retrograde degeneration. A stylised dorsal view of the brain displaying the routes of visual signal originating from the temporal and nasal parts of each eye with the corresponding visual fields was comprised from a number of sources and is provided on the left panel.[50–52] Pyramidal cells located in layer VI of the visual cortex are illustrated in green on the left hemisphere. These are the cells thought to contribute to signal feedback to the lateral geniculate nucleus (LGN) initiating retrograde degeneration from lesions caudal of the LGN. Black, numbered bars located in the right hemisphere represent possible positions of lesions associated with the correspondingly numbered visual field displayed on the middle panel. A detailed view inside the calcarine fissure (12) illustrates the anatomical areas corresponding to a congruous visual field defect. The visual field defect corresponding to a chiasmal lesion (3) can vary from a complete bitemporal hemianopia to central temporal visual field loss only (black area), if the lesion is limited to the caudal region of the chiasm. Based on the correlation of visual field and nerve fibre layer location, the most likely areas of nerve fibre layer thinning for each defect are indicated in the right panel. Predicted changes were compared to case studies reported in the literature (a: Huang-Link, Al-Hawasi and Eveman,[4] b: Shon and Sung,[26] c: Keller, Sanchez-Dalmau and Villoslada,[28] d: Meier and colleagues[29]). Note that all defects are shown for lesions in the right hemisphere, while left hemisphere lesions will result in side-inverted patterns. Ganglion cell loss is expected to mirror visual field defects for described lesions and was, therefore, not included. (Modified from J D Trobe 'The Neurology of Vision', Oxford University Press 2001, p 27).

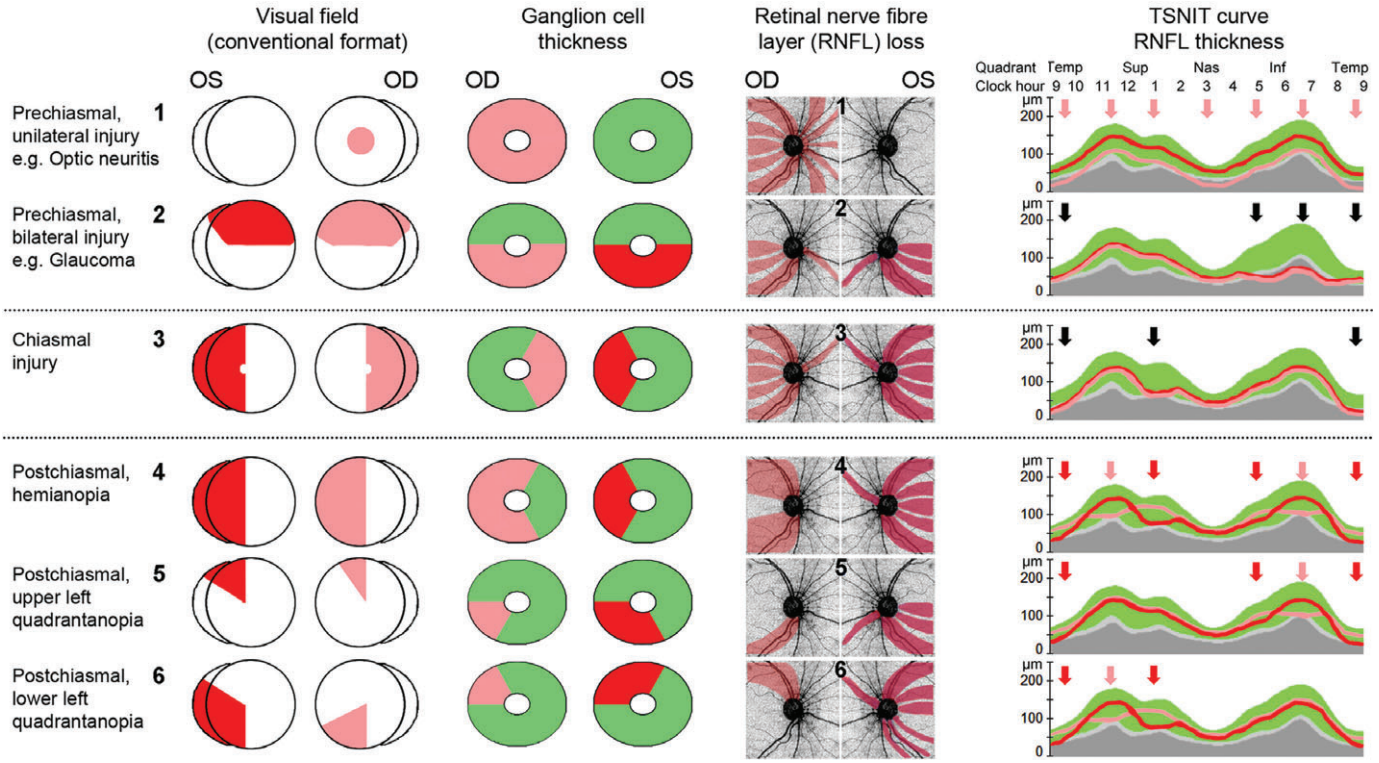

Figure 7. Schematic presentation of visual field deficits and corresponding ganglion cell and retinal nerve fibre loss. Schematic highlighting the relationship between visual field defects (conventional view), ganglion cell loss and changes in the retinal nerve fibre layer thickness. 1, 2. Pre-chiasmal changes are characterised by unilateral injury (1) or relatively symmetric bilateral changes (2) that obey the horizontal midline. 3. Insults in the chiasmal area result in bitemporal vision loss translating to mirrored changes in the ganglion and retinal nerve fibre layers leading to areas of bilateral depression in the temporal-superior-nasal-inferior-temporal (TSNIT) curve. 4–6. Post-chiasmal injuries are characterised by congruous visual field and ganglion cell changes that obey the vertical midline. The discordance to the presentation of nerve fibre loss is reflected in the notable asymmetry of retinal nerve fibre layer thinning highlighted by the TSNIT curve (red arrows indicate thinning of the respective eye, black arrows highlight areas of bilateral thinning).

optic neuropathies. The identification of retrograde or progressive nerve fibre degeneration is dependent on the time since insult, location of lesions and potential variations in the rate of degeneration. Diagnoses of the presented cases was reliant on high-resolution scans and partly the interpretation of their changes with respect to normative databases, as well as results from published investigations on the central 24–2 visual field.[37] As future information becomes available, we expect further refinement of the retinal nerve fibre layer reverse map. The ultimate step to optimise the plotting of retinal ganglion cells with different disorders may involve accrual of baseline data and individualised maps.[47]

The differentiation of optic neuropathies, particularly in the face of combined aetiologies and individual variations in the ganglion cell/nerve fibre layer complex, remains a clinical challenge. Systematic and comprehensive evaluation of clinical information enhances diagnostic acumen, as long as the clinician can differentiate useful from not-so-useful clinical information.[48,49] Therefore, adding to long standing criteria, we have developed an expanded and improved clinical reference (Figure 6) to aid in the differential diagnosis of optic neuropathies. Even in the absence of other tell-tale signs, a clinician armed with knowledge of the retinotopic organisation of axons entering the optic nerve head and carefully inspecting the OCT measures of the peripapillary nerve fibre layer may confidently suspect a signifying pattern of nerve fibre loss (Figure 7).

ACKNOWLEDGEMENTS

The authors extend particular thanks to the clinicians at CFEH, without whose exceptional expertise and efforts patient data collection and reviews would have been impossible.

This work was supported, in part, by a grant from the National Health and Medical Research Council (NHMRC) of Australia (1033224). Guide Dogs NSW/ACT is also a partner on the NHMRC grant and supplemented a PhD scholarship to Agnes Choi, who holds an Australian Postgraduate Award. Dr Zangerl holds a Faculty Research Grant awarded by the School of Optometry and Vision Science, University of New South Wales, Australia. Dr Kim was supported by an Australian Research Council (ARC) Future Fellowship (FT140100535).

REFERENCES

1. Hayreh SS. Ischemic optic neuropathy. *Prog Retin Eye Res* 2009; 28: 34–62.
2. Park HY, Park YG, Cho AH et al. Trans-neuronal retrograde degeneration of the retinal ganglion cells in patients with cerebral infarction. *Ophthalmology* 2013; 120: 1292–1299.
3. Pasol J. Neuro-ophthalmic disease and optical coherence tomography: glaucoma look-alikes. *Curr Opin Ophthalmol* 2011; 22: 124–132.
4. Huang-Link YM, Al-Hawasi A, Eveman I. Retrograde degeneration of visual pathway: hemimacular thinning of retinal ganglion cell layer in progressive and active multiple sclerosis. *J Neurol* 2014; 261: 2453–2456.
5. Jindahra P, Petrie A, Plant GT. The time course of retrograde trans-synaptic degeneration following occipital lobe damage in humans. *Brain* 2012; 135: 534–541.
6. Klistorner A, Sriram P, Vootakuru N et al. Axonal loss of retinal neurons in multiple sclerosis associated with optic radiation lesions. *Neurology* 2014; 82: 2165–2172.
7. Danesh-Meyer HV, Boland MV, Savino PJ et al. Optic disc morphology in open-angle glaucoma compared with anterior ischemic optic neuropathies. *Invest Ophthalmol Vis Sci* 2010; 51: 2003–2010.
8. Ambati BK, Rizzo JF 3rd. Non-glaucomatous cupping of the optic disc. *Int Ophthalmol Clin* 2001; 41: 139–149.
9. Piette SD, Sergott RC. Pathological optic-disc cupping. *Curr Opin Ophthalmol* 2006; 17: 1–6.
10. Zhang YX, Huang HB, Wei SH. Clinical characteristics of non-glaucomatous optic disc cupping. *Exp Therap Med* 2014; 7: 995–999.
11. Prum BE Jr, Rosenberg LF, Gedded SJ et al. Primary Open-Angle Glaucoma Preferred Practice Pattern guidelines. *Ophthalmology* 2016; 123: P41–P111.
12. Wong E, Yoshioka N, Kalloniatis M et al. Cirrus HD-OCT short-term repeatability of clinical retinal nerve fiber layer measurements. *Optom Vis Sci* 2015; 92: 83–88.
13. Golnik K. Non-glaucomatous optic atrophy. *Neurol Clin* 2010; 28: 631–640.
14. Xue K, Hildebrand GD. Retinal imaging: what the neurologist needs to know. *Pract Neurol* 2013; 13: 236–244.
15. Chiang J, Wong E, Whatham A et al. The usefulness of multimodal imaging for differentiating pseudopapilloedema and true swelling of the optic nerve head: a review and case series. *Clin Exp Optom* 2015; 98: 12–24.
16. Jamous KF, Kalloniatis M, Hayen A et al. Application of clinical techniques relevant for glaucoma assessment by optometrists: concordance with guidelines. *Ophthalmic Physiol Opt* 2014; 34: 580–591.
17. Simao LM. The contribution of optical coherence tomography in neurodegenerative diseases. *Curr Opin Ophthalmol* 2013; 24: 521–527.
18. Holmes G. The organizatin of the visual cortex in man. *Proc Roy Soc Lond Ser B* 1945; 132: 348–361.
19. Wong AM, Sharpe JA. Representation of the visual field in the human occipital cortex: a magnetic resonance imaging and perimetric correlation. *Arch Ophthalmol* 1999; 117: 208–217.
20. Ong YT, Hilal S, Cheung CY et al. Retinal neurodegeneration on optical coherence tomography and cerebral atrophy. *Neurosci Lett* 2015; 584: 12–16.
21. Sriram P, Graham SL, Wang C et al. Transsynaptic retinal degeneration in optic neuropathies: optical coherence tomography study. *Invest Ophthalmol Vis Sci* 2012; 53: 1271–1275.
22. Gabilondo I, Sepulveda M, Ortiz-Perez S et al. Retrograde retinal damage after acute optic tract lesion in MS. *J Neurol Neurosurg Psychiatry* 2013; 84: 824–826.
23. Trip SA, Schlottmann PG, Jones et al. Optic nerve atrophy and retinal nerve fibre layer thinning following optic neuritis: evidence that axonal loss is a substrate of MRI-detected atrophy. *NeuroImage* 2006; 31: 286–293.
24. Savino PJ, Danesh-Meyer HV. Retrochiasmal disorders. In: Rapuano CJ ed. Color Atlas & Synopsis of Clinical Ophthalmology: Neuro-Ophthalmology. Columbus, Ohio: McGraw-Hill Companies, Inc, 2003. pp 132–141.
25. Jindahra P, Petrie A, Plant GT. Retrograde transsynaptic retinal ganglion cell loss identified by optical coherence tomography. *Brain* 2009; 132: 628–634.
26. Shon K, Sung KR. Assessment of macular ganglion cell loss patterns in neurologic lesions that mimic glaucoma. *Korean J Ophthalmol* 2014; 28: 314–322.
27. Kardon RH. Role of the macular optical coherence tomography scan in neuro-ophthalmology. *J Neuro-ophthalmol* 2011; 31: 353–361.
28. Keller J, Sanchez-Dalmau BF, Villoslada P. Lesions in the posterior visual pathway promote trans-synaptic degeneration of retinal ganglion cells. *PloS One* 2014; 9: e97444.
29. Meier PG, Maeder P, Kardon RH et al. homonymous ganglion cell layer thinning after isolated occipital lesion: macular OCT demonstrates transsynaptic retrograde retinal degeneration. *J Neuro-ophthalmol* 2015; 35: 112–116.
30. Foroozan R. Chiasmal syndromes. *Curr Opin Ophthalmol* 2003; 14: 325–331.
31. Fujimoto N, Saeki N, Miyauchi O et al. Criteria for early detection of temporal hemianopia in asymptomatic pituitary tumor. *Eye* 2002; 16: 731–738.
32. Monteiro ML, Zambon BK, Cunha LP. Predictive factors for the development of visual loss in patients with pituitary macroadenomas and for visual recovery after optic pathway decompression. *Can J Ophthalmol* 2010; 45: 404–408.
33. Danesh-Meyer HV, Wong A, Papchenko T et al. Optical coherence tomography predicts visual outcome for pituitary tumors. *J Clin Neurosci* 2015; 22: 1098–1104.
34. Monteiro ML, Medeiros FA, Ostroscki MR. Quantitative analysis of axonal loss in band atrophy of the optic nerve using scanning laser polarimetry. *Br J Ophthalmol* 2003; 87: 32–37.
35. Jamous KF, Kalloniatis M, Hennessy MP et al. Clinical model assisting with the collaborative care of glaucoma patients and suspects. *Clin Exp Ophthalmol* 2015; 43: 308–319.
36. Asaoka R, Russell RA, Malik R et al. A novel distribution of visual field test points to improve the correlation between structure-function measurements. *Invest Ophthalmol Vis Sci* 2012; 53: 8396–8404.
37. Ferreras A, Pablo LE, Garway-Heath DF et al. Mapping standard automated perimetry to the peripapillary retinal nerve fiber layer in glaucoma. *Invest Ophthalmol Vis Sci* 2008; 49: 3018–3025.
38. Johnson H, Cowey A. Transneuronal retrograde degeneration of retinal ganglion cells following restricted lesions of striate cortex in the monkey. *Exp Brain Res* 2000; 132: 269–275.
39. Wong E, Yoshioka N, Kalloniatis M et al. Cirrus HD-OCT short-term repeatability of clinical retinal nerve fiber layer measurements. *Optom Vis Sci* 2015; 92: 83–88.
40. Heijl A, Buchholz P, Norrgren G et al. Rates of visual field progression in clinical glaucoma care. *Acta Ophthalmol* 2013; 91: 406–412.
41. Moon H, Yoon JY, Lim HT et al. Ganglion cell and inner plexiform layer thickness determined by spectral domain optical coherence tomography in patients with brain lesions. *Br J Ophthalmol* 2015; 99: 329–335.
42. Weinreb RN, Khaw PT. Primary open-angle glaucoma. *Lancet* 2004; 363: 1711–1720.
43. Wang H, Wu LL, Song XY et al. Axonal transport of BDNF precursor in primary sensory neurons. *European J Neurosci* 2006; 24: 2444–2452.
44. Balk LJ, Twisk JW, Steenwijk MD et al. A dam for retrograde axonal degeneration in multiple sclerosis? *J Neurol Neurosurg Psychiatry* 2014; 85: 782–789.
45. You Y, Gupta VK, Li JC et al. Optic neuropathies: characteristic features and mechanisms of retinal ganglion cell loss. *Rev Neurosci* 2013; 24: 301–321.
46. American Academy of Ophthalmology. Basic and Clinical Science Course: Neuro-Ophthalmology. Singapore, 2013–2014; section 5. San Francisco: American Academy of Ophthalmology, 2013.
47. Denniss J, Turpin A, McKendrick AM. Individualized structure-function mapping for glaucoma: practical constraints on map resolution for clinical and research applications. *Invest Ophthalmol Vis Sci* 2014; 55: 1985–1993.
48. Yoshioka N, Wong E, Kalloniatis et al. Influence of education and diagnostic modes on glaucoma assessment by optometrists. *Ophthalmic Physiol Opt* 2015; 35: 682–698.
49. Zangerl B, Hayen A, Mitchell P et al. Therapeutic endorsement enhances compliance with national glaucoma guidelines in Australian and New Zealand optometrists. *Ophthalmic Physiol Opt* 2015; 35: 212–224.
50. Biousse VR, Newman NJ. Neuro-ophthalmology Illustrated. New York: Thieme, 2009.
51. Reeves AG. Disorders of the Nervous System: a Primer. Chicago, Illinois: Year Book Medical Publishers, 1981; Chapter 3.
52. Kennard C, Leigh J. Neuro-Ophthalmology, Vol 102 (Handbook of Clinical Neurology). Available at: http://ezproxy.library.usyd.edu.au/login?url=http://www.sciencedirect.com/science/handbooks/00729752/129.

SUPPORTING INFORMATION

Additional supporting information may be found in the online version of this article at the publisher's website:

Figure S1. Variations of clinical findings with glaucoma.

Table S1. Glaucoma patients' characteristics. All lesions were located in the optic nerve head.